

## Nanotube Synthesis

# A Facile Way to Control the Number of Walls in Carbon Nanotubes through the Synthesis of Exposed-Core/Shell Catalyst Nanoparticles\*\*

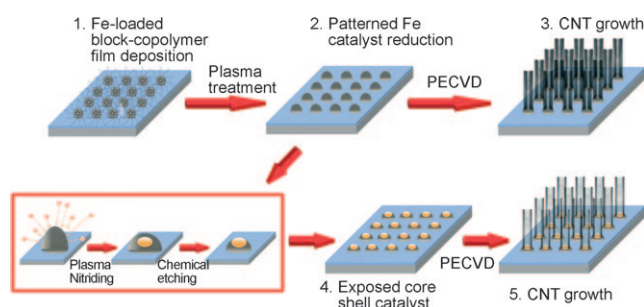
Kyung Min Choi, Saji Augustine, Jung Hoon Choi, Ju Ho Lee, Weon Ho Shin, Seong Ho Yang, Jeong Yong Lee, and Jeung Ku Kang\*

There is currently great interest in the controlled synthesis of carbon nanotubes (CNTs) with unique structures.<sup>[1–3]</sup> Much of this attraction lies in the fact that the functionality of CNTs can be significantly tailored by control of their composition, diameter, and number of walls. CNTs are known to act as either metals or semiconductors, depending on their diameters and chiralities,<sup>[4,5]</sup> for example; therefore, precise control of their nanostructures is essential for various applications, such as field-emitter tips in displays,<sup>[6]</sup> transistors,<sup>[7]</sup> interconnection and memory elements in integrated circuits,<sup>[8]</sup> scan tips for atomic force microscopy,<sup>[9]</sup> and energy-storage media.<sup>[10]</sup>

One conventional method for growing vertically aligned CNTs involves the use of chemical vapor deposition (CVD). In this case, CNTs can be grown selectively on catalytic sites and their properties depend to a large extent on the nanostructure of the catalyst, particularly the particle size, interparticle distance, and composition.<sup>[11,12]</sup> It is therefore necessary to develop improved catalysts using highly innovative methods in order to obtain desired CNT functionalities. Traditional methods for designing and preparing catalyst particles to control the properties of CNTs include a metal film sputtering method,<sup>[13,14]</sup> an organic silica mesoporous template method,<sup>[15]</sup> a nanoparticle method,<sup>[16–18]</sup> and a self-assembled block copolymer template method.<sup>[19–22]</sup> These methods, however, only focus on controlling the diameter or interparticle distance of CNTs by controlling the size or interparticle distance of the catalyst particles. While it has been reported that controlling the number of walls in CNTs is possible by adjusting the catalyst size, some limitations remain with respect to controlling the diameter and number of walls simultaneously. This suggests that CNT nanostructures with required diameters and interlayer walls cannot be adequately controlled with current methods, and that a new innovative technique for controlling the diameter and the number of CNT walls simultaneously is required.

Herein we report a facile way of controlling the number of CNT walls and their diameters simultaneously by using exposed-core/shell (ECS) catalysts composed of catalytically active iron in the shell layer and inactive iron nitride in the exposed core area. As these ECS catalysts were prepared using an Fe-loaded diblock copolymer micelle to pattern the nanoparticles in a controllable manner,<sup>[23]</sup> this approach provides a total solution for controlling the CNT alignment and pattern as well as its nanostructure simultaneously.

The synthetic process is illustrated in Scheme 1. Thus, after synthesizing the diblock copolymer micelle solution, Fe precursors were loaded into the micelle core. This Fe-loaded micelle solution was then coated onto a Si/SiO<sub>2</sub> substrate in a spin-coater to give a hexagonally arrayed pattern of micelles.<sup>[23]</sup> Subsequent low-temperature plasma treatment resulted in the formation of metal particles upon reduction of the metal precursors in the micelle core and removal of the micelle polymers. The resulting Fe nanoparticles patterned on a substrate were placed in a nitrogen plasma to precipitate the iron nitride inside each particle at high temperature. After this precipitation step, a chemical etching process was followed to remove the outer part of the iron shell and expose the iron nitride core. The resulting ECS catalysts, which are composed of an exposed core area (catalytically inactive) and a shell layer (catalytically active), were found to be arranged on the substrate with a constant size and interparticle distance.



**Scheme 1.** The exposed-core/shell (ECS) catalyst used to simultaneously control the number of walls and diameter of CNTs. Fe-loaded micelles are coated onto the substrate with a spin coater, which gives rise to a hexagonal arrangement of metal precursors. The Fe-loaded micelles are then treated with plasma to form patterned Fe nanoparticles at relatively low temperature. The ECS catalysts are synthesized by plasma treatment at high temperature and chemical etching of the patterned substrate in order to precipitate the iron nitride in the Fe particles and to expose the iron nitride core, respectively. Two kinds of CNTs are grown in the MPECVD using both pure pristine Fe catalysts and ECS catalysts and compared to determine the effects of ECS particles.

[\*] K. M. Choi, S. Augustine, J. H. Choi, J. H. Lee, W. H. Shin, S. H. Yang, Prof. J. Y. Lee, Prof. J. K. Kang  
NanoCentury KI and  
Department of Materials Science & Engineering, KAIST  
373-1, Guseong-dong, Yuseong-gu, Daejeon 305-701 (Korea)  
E-mail: jeungku@kaist.ac.kr

[\*\*] This work was supported by grant no. M103KW010017-06K2301-01720 from the Hydrogen Energy R & D program, which is itself funded by MEST (grant no. R0A-2007-000-20029-0), and by a Korean Research Foundation Grant (KRF-2005-005J09703).

Supporting information for this article is available on the WWW under <http://dx.doi.org/10.1002/anie.200803311>.

Two different kinds of CNTs were grown by this microwave plasma enhanced chemical vapor deposition (MPECVD) method using both pure, pristine Fe catalysts and ECS catalysts and compared in order to study the effect of the ECS catalysts on CNT structure. It was found that the ECS catalysts can selectively control the number of CNT walls without affecting any of the CNTs' other characteristics, such as their diameters, lengths, or alignments. Since the overall process is composed of consecutive processes including application of nanotemplate micelles, catalyst deposition by spin coating, nanotemplate treatment in a nitrogen plasma, and CNT growth by MPECVD, this novel approach should be readily scalable to macroscopic scales and should be suitable for controlling the number of walls in a large quantity of CNTs.

Scanning electron microscopy (SEM), atomic force microscopy (AFM), and transmission electron microscopy (TEM) images of pristine and ECS catalysts are shown in the left and right panels of Figure 1, respectively. The pristine catalyst nanoparticles formed on the substrate have a uniform size (ca. 15 nm) and distribution (Figure 1 a). This is because the size of the catalyst particles is defined by the core size of the micelle and the metal precursor concentration, whereas their lateral distribution over large areas is controlled by the whole size of the micelles. The pristine catalyst particles are also presented as 3D topographical (Figure 1 c) and phase images (Figure 1 e), obtained by AFM in the tapping mode, which show that their shape is clearly hemispherical and their constitution uniform. Although some contrast differences can be seen around all the particles in the AFM phase image, these are due to a topographical effect induced by abrupt changes in their height rather than by a phase difference.

The pristine catalysts were compared directly with the ECS catalysts in terms of shape, size, and local compositional differences. In the case of ECS particles, there is an obvious difference in the contrast between the exposed core region and the shell region in a particle (Figure 1 b), due to the formation of iron nitride at the center of the particle. They are essentially the same size as the pristine particles, however, despite suffering from surface smoothing during the chemical etching process. The topographical AFM image of ECS catalyst particles (Figure 1 d) shows that the particles retain a hemispherical morphology, which indicates that the difference between pristine and ECS particles is not induced by morphological changes. The contrast difference due to the exposed core of the ECS particles in the AFM phase image (Figure 1 f) indicates that there is some phase or constitutional change induced by iron nitride precipitation in the exposed core region; the shell region remains the same. The high resolution TEM (HRTEM) images (Figure 1 g,h) confirm the presence of an exposed iron nitride core in the ECS particle. The (111) spacings for the upper area of the pristine and ECS catalyst particles obtained from the two cross-sectional HRTEM images along the  $[110]_{\text{Si}}$  zone axis are 0.208 and 0.210 nm, respectively. These values match those obtained from the crystallographic data in the ICSD (Inorganic Crystal Structure Database) exactly. The lattice parameter differences were further confirmed by fast Fourier transformation (FFT; insets in Figure 1 g,h). The red and

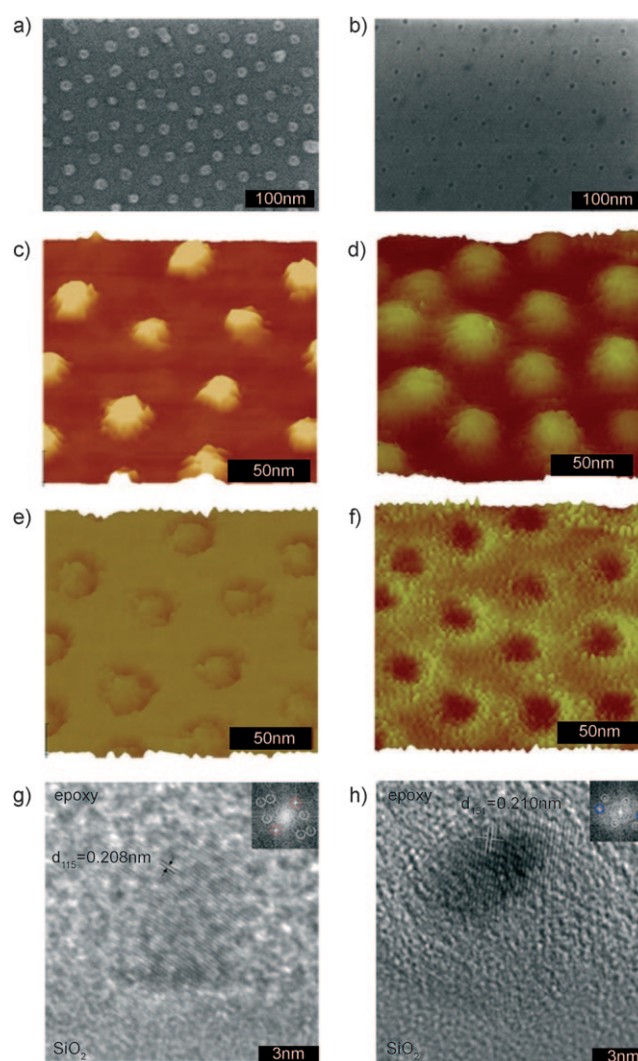


**Figure 1.** High-magnification SEM image of a) patterned iron catalyst nanoparticles without any further treatment and b) exposed-core/shell structured (ECS) catalysts after nitrogen plasma treatment and chemical etching. The average size of both catalysts is about 15 nm. c,d) 3D topographical AFM images (tapping mode) of pristine and ECS catalysts, respectively. e,f) 3D phase AFM images of pristine and ECS catalysts, respectively. The constitution of the catalyst is changed by plasma nitriding treatment without morphological change in the ECS catalyst. g,h) HRTEM and FFT images (inset) of pristine and ECS catalysts, respectively, which show the presence of iron nitride at the upper part of an ECS catalyst particle by means of the lattice parameter and contrast difference.

blue circles in the FFT images represent the (111) planes of iron and iron nitride, respectively.

Formation of the iron nitride core of the ECS nanoparticles is induced by nitrogen plasma treatment. This occurs similar to a well-understood thermochemical engineering process by which nitrogen is introduced into the region of ferritic iron-based (steel) workpieces at high temperature. It has been widely reported that iron nitride can be precipitated near the surface of iron by holding it in a nitrogen plasma; this process is known as plasma nitriding.<sup>[24–26]</sup> As the structure and formation mechanism of the ECS nanoparticles was clear

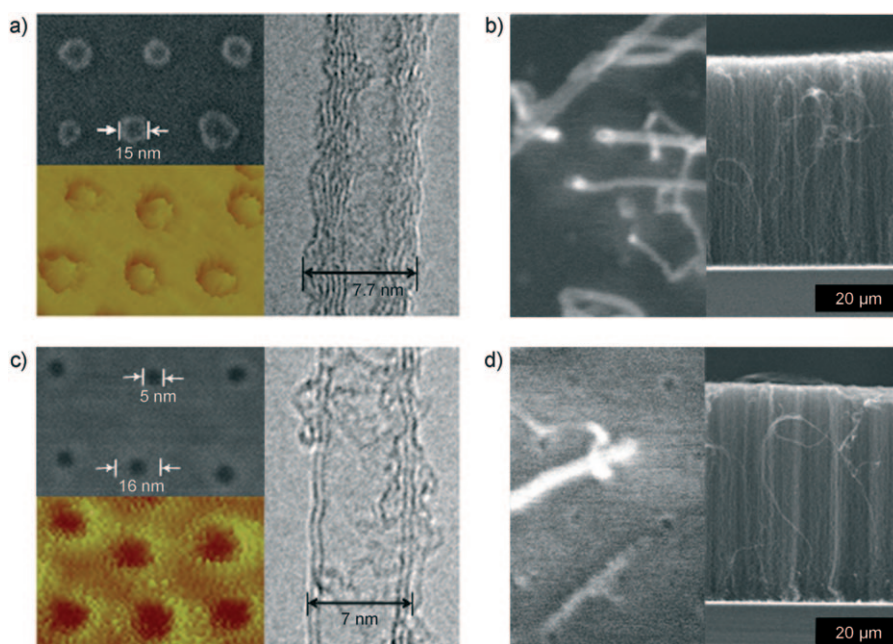


**Figure 2.** Image showing the catalyst size (SEM) and structure (AFM), along with the diameter and number of walls in the CNTs, for a) pristine and c) ECS catalysts. The formation of a catalytically inactive iron nitride core at the center of the catalyst alters the number of walls in the CNTs independently of their diameter (7–8 nm). b,d) SEM images of CNTs grown vertically from pristine (b) and ECS (d) catalysts in plain (left) and cross-sectional view (right). The length of the CNTs formed from both catalysts is about 48  $\mu\text{m}$ , therefore only the number of walls is exclusively controlled by the ECS catalyst.

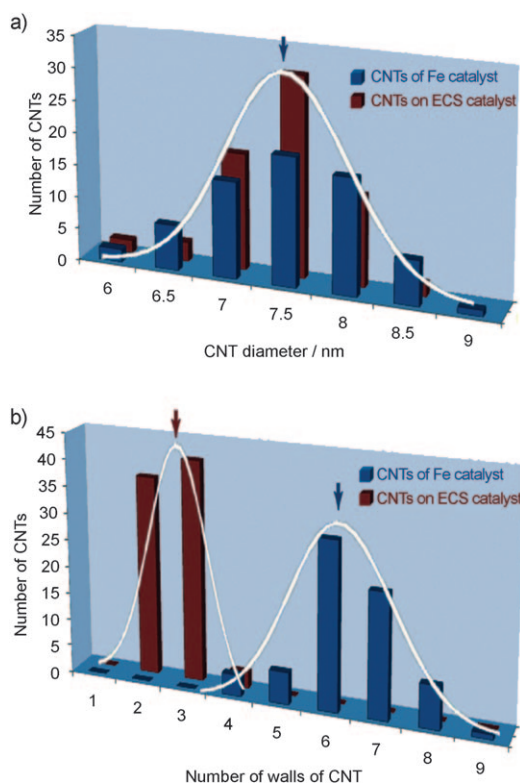
from the images in Figure 1, it appeared worthwhile to study how they affect the structure of CNTs.

Figure 2 shows a comparison of CNTs and their catalysts in terms of diameter and structure. This comparison clearly shows that the ECS catalyst affects the number of walls of the CNTs without any other effects. It is well known that the diameter of CNTs grown by CVD methods is closely related to the sizes of the catalyst, therefore the diameters of CNTs (Figure 2a,c) grown from both pristine and ECS catalysts are similar to each other (7.7 and 7.0 nm, respectively) and almost half the size of the catalyst particles (ca. 15 nm). The number of walls in the CNTs is reduced from six or seven for those synthesized with the pristine catalyst to two or three for those synthesized with the ECS catalyst; all are highly uniform (Figure 2a,c). The inner diameter of the CNTs grown from the ECS catalyst (5.05 nm) corresponds almost exactly to the size of the iron nitride core of the ECS catalyst (5.0 nm), which does not catalyze CNT growth. While the diameter of the CNT is determined by the size of the catalyst, the catalytically inactive iron nitride core at the center of the catalyst determines the number of walls in the CNTs by restricting the growth of the CNT's inner walls. The growth process of the CNTs proceeds according to the following sequence of steps: 1) a hydrocarbon such as methane adsorbed onto the catalytic particle's surface releases carbon upon decomposition, which dissolves and diffuses into the particle; 2) when a supersaturated state is reached, carbon precipitates in a crystalline tubular form.<sup>[27]</sup> In the case of ECS catalyst particles, the iron nitride core cannot catalyze the precipitation step required for CNT growth, therefore the

exposed cores of the catalyst particles control the number of CNT walls with constant diameter. The left side of Figure 2b,d shows plain-view SEM images after removal of some CNTs grown from the substrate; the images show remaining catalysts. These images indicate that the CNTs are formed by bottom-up growth and that the ECS catalysts retain their structures during CNT synthesis by MPECVD. The images on the right side of Figure 2b,d show cross sections of the CNTs grown on the substrate. In both cases, the CNTs grow vertically and their lengths are about 48  $\mu\text{m}$ . This confirms that an ECS catalyst particle has catalytic activity and that the CNT growth mechanism is similar to that with the pristine catalyst. The number of walls is therefore exclusively controlled by the ECS particles during the growth process while the diameters and lengths of the CNTs remain constant, as shown in Figure 2.

Figure 3 summarizes the statistical analysis for the diameters and number of CNT walls, which were obtained for 70 CNTs from a wide selection of TEM images (see the Supporting Information). Figure 3a shows that the diameter distributions (ca. 7.5 nm) for CNTs obtained from both the pristine and ECS catalysts are almost identical. This is because the diameter of the CNTs is controlled by the catalyst size, which is identical in both cases. The distribution of the number of CNT walls is shown in Figure 3b (see also Figure 2), where it can be seen that the number of CNT walls is generally two or three for CNTs formed from an ECS catalyst but six or seven for those formed from a pristine catalyst.

In conclusion, we have demonstrated a facile method for controlling the number of walls of CNTs without altering any other characteristics that involves the synthesis of ECS catalyst nanoparticles. We have synthesized ECS catalysts composed of an exposed iron nitride core and an iron shell and have demonstrated the effect of these ECS catalysts on the number of walls in the resulting CNTs by comparing CNTs grown from ECS and pristine Fe catalysts. The main factor that controls the number of walls in the CNTs is a combination of the confined size of the catalyst and the catalytically inactive iron nitride core. Thus, while the confined size of the catalysts controls the diameter of the CNTs, the number of their inner walls is controlled by the catalytically inactive iron nitride at the exposed core of the catalysts. A precise control over the arrangement and pattern of CNTs, as well as the diameter and number of walls, is expected to be feasible using this approach by modifying the composition of the diblock-copolymer micelles. This



**Figure 3.** a) Statistical size distribution of CNTs obtained from pristine Fe and ECS catalysts. The diameter distribution of the CNTs is almost the same due to the identical size of the catalysts in both cases. b) Statistical wall distribution of CNTs obtained from pristine Fe and ECS catalysts. The number of walls in the CNTs varies upon catalyst modification due to the formation of a catalytically inactive iron nitride core at the center of the Fe catalysts.

approach may therefore be useful for designing new nanoscale catalysts and the catalytic growth of other nanomaterials, which could open up the fascinating possibility of device integration and hydrogen storage for various nanomaterials.

### Experimental Section

The asymmetric diblock copolymer polystyrene-*block*-poly(4-vinylpyridine) (PS-P4VP) was purchased from Polymer Source Inc. The number average molecular weights of PS and PVP were 47600 and 20600  $\text{g mol}^{-1}$ , respectively. The polydispersity index was 1.14. Nitric acid and iron chloride were purchased from Aldrich Chemical Co. The microwave plasma enhanced chemical vapor deposition (MPECVD) system was purchased from Woosin Cryovac Ltd.

For a free-standing monolayer film of diblock copolymer micelles, micellar solutions were prepared by dissolving monodisperse PS-P4VP in toluene to yield a 0.5 wt% solution. Ferric chloride ( $\text{FeCl}_3$ ), which was employed as a precursor of the iron nanoparticles, was added to this 0.5 wt% toluene solution of PS-PVP micelles ( $\text{FeCl}_3/\text{vinylpyridine}$  molar ratio: 0.5) and stirred for at least 24 h. A monolayer film of the resulting hexagonal micelles was coated in a spin coater at 2000 rpm followed by nitrogen plasma treatment (800 W, ca. 14 Torr) at 100 °C for 90 s to fabricate an array of iron oxide nanoparticles on the  $\text{SiO}_2/\text{Si}$  substrate. The substrate was then treated with nitrogen plasma again (800 W, ca. 14 Torr) at 800 °C for 60 s to precipitate iron nitride in the iron oxide particle. The substrate was then submerged in 30 mL of a solution of nitric acid and ethanol (1:3 v/v) for 2.5 h.

The CNTs were synthesized by microwave plasma enhanced chemical vapor deposition (MPECVD). The substrate was first evacuated and heated to 700 °C. The chamber was then charged with 12 Torr  $\text{H}_2$ , and  $\text{H}_2$  plasma treatment of the substrate to reduce the iron oxide was conducted for 3 min. The CNTs were then prepared by catalytic decomposition of  $\text{CH}_4$  as carbon source gas in the MPECVD apparatus in a 21-Torr mixture of  $\text{H}_2$  and  $\text{CH}_4$  for 10 min. The growth rate of the CNTs was approximately 4.8  $\mu\text{m min}^{-1}$ .

Received: July 8, 2008

Published online: October 16, 2008

**Keywords:** chemical etching · core-shell structures · materials science · nanotubes · plasma chemistry

- [1] H. J. Dai, E. W. Wong, C. M. Lieber, *Science* **1996**, 272, 523.
- [2] P. M. Ajayan, T. W. Ebbesen, *Rep. Prog. Phys.* **1997**, 60, 1025.
- [3] S. J. Kang, C. Kocabas, T. Ozel, M. Shim, N. Pimparkar, M. A. Alam, S. V. Rotkin, J. A. Rogers, *Nat. Nanotechnol.* **2007**, 2, 230.
- [4] T. W. Odom, J.-L. Huang, P. Kim, C. M. Lieber, *Nature* **1998**, 391, 62.
- [5] T. W. Wilder, L. C. Venema, A. G. Rinzler, R. E. Smalley, C. Dekker, *Nature* **1998**, 391, 59.
- [6] S. S. Fan, M. G. Chapline, N. R. Franklin, T. W. Tomblor, A. M. Cassell, H. J. Dai, *Science* **1999**, 283, 512.
- [7] a) S. J. Tans, C. Dekker, *Nature* **2000**, 404, 834; b) P. L. McEuen, M. S. Fuhrer, H. K. Park, *IEEE Trans. Nanotechnol.* **2002**, 1, 78.
- [8] J. H. Hafner, C. L. Cheung, A. T. Woolley, C. M. Lieber, *Prog. Biophys. Mol. Biol.* **2001**, 77, 73.
- [9] H. J. Dai, J. H. Hafner, A. G. Rinzler, D. T. Colbert, R. E. Smalley, *Nature* **1996**, 384, 147.
- [10] A. C. Dillon, K. M. Jones, T. A. Bekkedahl, C. H. Klang, D. S. Bethune, M. J. Heben, *Nature* **1997**, 386, 377.
- [11] J. Kong, H. T. Soh, A. M. Cassell, C. F. Quate, H. Dai, *Nature* **1998**, 395, 878.
- [12] C. Laurent, E. Flahaut, A. Peigney, A. Rousset, *New J. Chem.* **1998**, 22, 1229.
- [13] L. Delzeit, C. V. Nguyen, B. Chen, R. Stevens, A. Cassell, J. Han, M. Meyyappan, *J. Phys. Chem. B* **2002**, 106, 5629.
- [14] A. J. Hart, A. H. Slocum, L. Royer, *Carbon* **2006**, 44, 348.
- [15] R. Gras, J. L. D., T. Minéa, M. Dubosc, P. Y. Tessier, L. Cagnon, P. Coronel, J. Torres, *Microelectron. Eng.* **2006**, 83, 2432.
- [16] H. Ago, S. Imamura, T. Okazaki, T. Saito, M. Yumura, M. Tsuji, *J. Phys. Chem. B* **2005**, 109, 10035.
- [17] R. Y. Zhang, I. Amlani, J. Baker, J. Tresek, R. K. Tsui, P. Fejes, *Nano Lett.* **2003**, 3, 731.
- [18] W. E. Alvarez, F. Pompeo, J. E. Herrera, L. Balzano, D. E. Resasco, *Chem. Mater.* **2002**, 14, 1853.
- [19] M. Park, C. Harrison, P. M. Chaikin, R. A. Register, D. H. Adamson, *Science* **1997**, 276, 1401.
- [20] W. A. Lopes, H. M. Jaeger, *Nature* **2001**, 414, 735.
- [21] M. T. Tuominen, T. P. Russell, *Science* **2000**, 290, 2126.
- [22] D. H. Lee, D. O. Shin, W. J. Lee, S. O. Kim, *Adv. Mater.* **2008**, 20, 2480.
- [23] B. H. Sohn, S. I. Yoo, B. W. Seo, S. H. Yun, S. M. Park, *J. Am. Chem. Soc.* **2001**, 123, 12734.
- [24] G. Miyamoto, Y. Tomio, T. Furuhashi, T. Mak, *Mater. Sci. Forum* **2005**, 539, 492.
- [25] D. Hovorka, J. Vleček, R. Čerstvý, J. Musil, P. Bělský, M. Růžička, J. G. Han, *J. Vac. Sci. Technol. A* **2000**, 18, 2715.
- [26] S. L. Semiatin, *Metalworking: bulk forming/prepared under the direction of the ASM International Handbook Committee*, Vol. 14, ASM International, **2005**.
- [27] M. Meyyappan, et al., *Plasma Sources Sci. Technol.* **2003**, 12, 205.